Journal of Optoelectronics and Advanced Materials, Vol. 3, No. 2, June 2001, p. 563 - 570

ANALYSIS OF a-SiO_2/ a-Si MULTILAYER STRUCTURES BY ION BEAM METHODS AND ELECTRON SPIN RESONANCE

N. Tomozeiu[a], J. J. van Hapert, W. M. Arnoldbik, E. E. van Faassen, A. M. Vredenberg, F. H. P. M. Habraken

Debye Institute, Utrecht University, PO Box 80000 3508 TA, Utrecht, The Netherlands
[a]Faculty of Physics, Bucharest University, PO Box 11Mg, Bucharest-Magurele, Romania

Multilayered structures of a-Si/SiO_2 sequences were deposited using a magnetron sputtering system, where Si atoms are sputtered in an Ar-O_2 mixture. All samples have the same total thickness (250nm) and the thickness/layer is between 2 nm and 16 nm. The purpose of this paper is to investigate the inhomogeneity of these films and its limit. The sample composition and thickness were investigated by conventional Rutherford backscattering spectrometry (RBS), high resolution RBS using a magnetic spectrograph and elastic recoil detection (ERD). The analysis of the conventional RBS and ERD spectra has revealed that samples with 16 nm/layer consists of a-Si/SiO_2 sequences. The high-resolution RBS measurements have also shown a multilayered structure for samples with a smaller layer thickness. The composition of the SiO_2 layers for samples with 4 and 2 nm/layer is more SiO_x like, with different values of the x parameter. It seems that the interface region is dominant for these samples with 4 nm/layer and less. The structural study is completed with the ESR measurements, which revealed two paramagnetic species attributed to a-Si dangling bonds and E' centers respectively. The latter are characteristic for SiO_2 material. We found that a-Si DBs are present in all samples, irrespective of the layers thickness. Their spin density amounts to about $10^{20}cm^{-3}$. In contrast, the E' centers are not present in the sample with 2 nm/layer.

(Received May 20, 2001; accepted June 11, 2001)

Keywords: Multilayer structure, a - SiO_2/a - Si, ESR, Ion beam methods

1. Introduction

The era of nano-technologies and nano-devices offers challenging fields to scientists. As a result, in the last decade many studies have been devoted to multilayered structures of amorphous semiconductors. There is an equal interest in these layered films for both fundamental physics and applications. A very interesting aspect is how the structure of each layer from the stack influences the physical properties of the complete structure. Some amorphous materials from the chalcogenide glass family (e.g. InSe) show particularities as each layer is formed in sublayers in a well-known sequence (e.g. Se-In-In-Se) /1/. Materials from the family of silicon are structurally organized within a tetrahedral basic cell built around a silicon atom. The Si-Si_4 structure has Si-Si bond length of 2.38Å while Si-O_4 is characterized by Si-O bond of 1.66Å /2/. This mismatch at the SiO_2/Si interface, in a structure with thin layers, will play an important role in the behavior of the microelectronic devices.

One very important step in the structural study is the compositional determination with a high accuracy. Using the ~ MeV ion-beam analysis techniques, the elemental composition of layers can be probed as a function of depth by analyzing the spectra of scattered or recoiled ions. The typical depth resolution near the surface varies from 5-10 nm for conventional methods to better than 1 nm using a dedicated high resolution instrument. The concentration of the atoms of which a thin layer consists can be obtained on an absolute scale. No information is obtained about the chemical environment of the probed atoms. The most popular ion-beam analyses techniques used to investigate semiconductor layers are Rutherford backscattering spectrometry (RBS) and elastic recoil detection (ERD).

The nature and the quantity of defects from the material structure are also very important for structural characterization. Electron spin resonance (ESR) is a technique used to determine the paramagnetic dangling bond defects.

In this paper we present results of ion beam analyses methods and ESR on a-SiO_2/a-Si multilayer structures. Combining the RBS and ERD results with those from ESR measurements we will find a limit where the a-SiO_2/a-Si sequences can be resolved.

2 Experimental

2.1. Sample preparation

Multilayers of a-SiO_2/a-Si were deposited in a sputtering system equipped with a 13.56 MHz r.f. magnetron source using a power of 140 W. The deposition chamber was pumped down to a base pressure of less than $2\cdot10^{-7}$ mbar before the plasma gas was introduced. Silicon atoms were sputtered from a polycrystalline silicon target. When the SiO_2 layers were deposited, the oxygen line was opened. The ratio between Ar and O_2 flows was 80:1. For the next a-Si layer the oxygen line was closed while the plasma runs continuously with the same argon flow. In this way samples with 2, 4, 8 and 16 nm/layer were deposited. In order to obtain sharper interfaces, samples with a layer thickness of 2 nm and 4 nm were also deposited by a procedure in which for each layer the following steps have been done: i) a basis pressure of $2\cdot10^{-7}$ mbar; ii) the plasma gasses were introduced (the ratio Ar/O was 80/1 for SiO_2 layers and for a-Si layers was 80/0); iii) turn on the plasma and keep it to obtain the desired thickness. We denote these samples as "plasma on/off" and the first series of samples as "plasma on". During deposition the pressure was 5.6 μbar. The distance between target and sampler holder is 6 cm. All samples were deposited on both c-Si wafer (for ion beam analyses) and corning glass (for ESR) at room temperature.

2.1. Measurement techniques

Rutherford Backscattering Spectrometry uses a beam of light ions, usually He or H, with high energy (0.5 – 3 MeV), which scatter from the nuclei in the measured layer (target) /3/. The number and energy of scattered ions, usually at a backward angle, in the direction of a particular detector are determined. RBS is used with success to determine the concentration depth profiles of heavy atoms in a matrix of light atoms. The relations between the energies and mass numbers for elastic scattering is determined by the kinematics of the collision. An important parameter is the stopping power defined as the energy loss divided by the atomic areal density of the target (eV/(10^{15} at/cm^2)). This parameter determines the depth sensitivity and the depth resolution. The stopping cross section data have been collected in the Ziegler's tables /4/. Due to the statistical nature of the stopping process the amount of energy lost per unit length fluctuates. For a path length *t* this spread, called energy straggling increases, with $t^{1/2}$. The RBS spectra are analyzed using a computer program which calculate the spectra for an assumed sample composition taking into account the effects of straggling, detector resolution, multiple scattering, etc /5/. Comparing the calculated spectra with the measured one, in successive approximation the absolute concentration depth profiles for elements from the sample are obtained.

Fig. 1 shows the RBS spectra for a SiO_2 thin film deposited by sputtering on c-Si. The depth resolution near the surface is determined by the detector resolution (15 keV), while at a larger depth, de resolution is mainly determined by energy straggling. In this figure the contributions of Ar, a heavier element than Si (the host matrix) and of O a lighter element are well visible. We have to note that the RBS sensitivity is poor for light elements ($\sigma_{RBS} \sim Z^2$, σ is the cross section that characterize the collision event, Z is the atomic number). Also RBS based on He ions has a limited mass resolution and it is difficult to resolve isotopes or neighbouring elements. The solutions for this problems are given by ion-beam analyses techniques by ERD and high resolution RBS (HR-RBS).

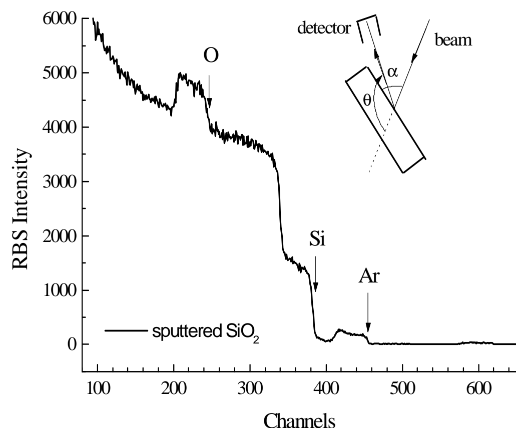

Fig. 1. The RBS spectrum of SiO_2 layer deposited on c-Si. The position of the surface edges for Si, O, N and Ar are indicated. The primary beam consisted of 2 MeV He^+ ions.

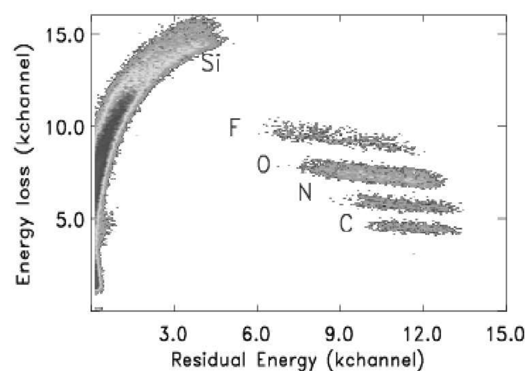

Fig 2. ERD spectra of a contaminated SiO_x layer measured with a ΔE-E ionization chamber. The separation between elements and the depth for each element are revealed.

Elastic Recoil Detection (ERD) uses the information about the collision between the incident ion and the target atoms contained in recoiled ions. Because momentum is conserved, the detection necessarily occurs at forward angles. The advantages of RBS are preserved by ERD (good quantitative character, depth resolution, non-destructive technique) and more, the sensitivity for light elements is strongly enhanced. In ERD heavy ion (Si, Ag, Cu) beam of tens of MeV's are used. The ERD setup at Utrecht University is connected to a 6 MeV EN Tandem Van de Graaff Accelerator. A ΔE-E ionization chamber with Frisch grid is used as detector /6/. The entrance window of the detector is a 2 μm metalized Mylar foil which separates the 24 mbar iso-butane in the ionization chamber from the vacuum in the scattering chamber. The anode of the detector is composed of two segments: a 6 cm segment for ΔE signal and a 17 cm segment for the E signal. In this way a total energy spectrum for each light element is constructed from a two-dimensional ΔE-E spectrum. The depth resolution is comparable with the resolution obtained with RBS but the mass separation is enhanced. Figure 2 shows an example of ERD spectrum for a contaminated SiO_x layer. Elements as C, N, O, F and Si are well separated. The number of atoms per cm^2 of the light elements in the film is obtained by comparing the yields in the different features with those of a reference thin film with a known abundance of one of the light elements. When no spectral overlap occurs, the minimum detectable amount of the considered elements is better than 10^{13} $at.cm^{-2}$.

High Resolution RBS (HR-RBS) spectra can be obtained using a magnetic spectrograph also installed at Utrecht University. It consists of a quadrupole lens, a Wien filter and a 90° dipole magnet with field corrections. The setup from Utrecht University was built in such a way that the spectrograph together with the main chamber (UHV chamber) can be rotated along a circular rail within 0° and 120°. The chamber is connected with a transfer system with a preparation chamber equipped with a load-lock facility. The fields in the components of the spectrograph can be set by a computer and can be tuned to select one ion species with given mass and charge to pass through the spectrograph. A two-dimensional position-sensitive detector (energy versus angle) images one charge state of a selected ion species scattered from the sample. An energy range of 10% of the nominal energy E is resolved with an energy resolution ΔE/E of 9×10^{-4} that can be translated into a depth resolution at the surface of 6Å /7/.

For comparison, we propose the spectra of the same multilayered sample (a-Si/SiO_2 with 8 nm/layer) obtained with conventional RBS (figure 3) and HR-RBS (figure 5). The first spectrum does no show any multilayered structure, the HR-RBS spectrum reveals the 8 nm of a-Si and SiO_2 respectively. The depth resolution of HR-RBS allows to determine the composition and the thickness of each layer from the structure.

To analyze our samples we used these three techniques in the following circumstances: i) The conventional RBS measurements were done with a 2.4 MeV He^+ beam. The angle between the incoming beam and the sample surface was α=65^0. The detector was placed under an angle of θ=120^0 with the beam direction. ii) ERD measurements were performed using a primary beam of 50 MeV Cu^{+9} incident at 20° with the surface of the sample and a recoil angle of 30°. iii) in HR-RBS a He^+ beam of 800 keV in a configuration with α=35^0 and θ=140^0 was used.

The structural study was completed with ESR measurements that were performed using a Bruker ESP 300 system. All samples were measured at room temperature and the microwave power was 1.68mW.

3. Results and discussions

3.1. Ion beam analyses

The conventional RBS spectra of multilayered a-Si/SiO_2 samples with 2, 4, 8 and 16 nm/layer are shown in Fig. 3. From this figure it is deduced that silicon, oxygen and argon are present in the layer structure. From previous experiments on single layers we know that the argon concentration is 1.6% for SiO_2 layers and 2.9% for a-Si. Its presence in the layer is explained by implantation of argon ions from the plasma during deposition. As can be seen, only the spectrum of the sample with layer thickness of 16 nm presents a multilayered structure. The simulation using the RUMP computer code confirms the composition of a-Si and SiO_2. Because of the limited depth resolution, all other samples with a layer thickness up to 8 nm have an unresolved RBS spectrum. All these spectra are similar with spectra of single a-SiO_x layers, i.e. x is averaged over all layers from the deposited stack. For sequences of a-Si/SiO_2 this average value of x should be the same indifferently on the individual layer thickness. As Fig 3 shows and the simulation confirms, <x> decreases with decreasing the layer thickness. This means that the SiO_2 composition changes into SiO_x and/or the interface layer has a dominant contribution. Similar results are obtained from ERD measurements as Fig. 4 shows. Because in ERD no interfering background signal is present, small changes of the oxygen contents can be determined. As we have seen in the previous chapter the ERD depth resolution for thin films is about 10 nm. Therefore, the multilayered structures with smaller layer thickness can not be seen, but the advantage of the method is a more accurate determination of the <x> value.

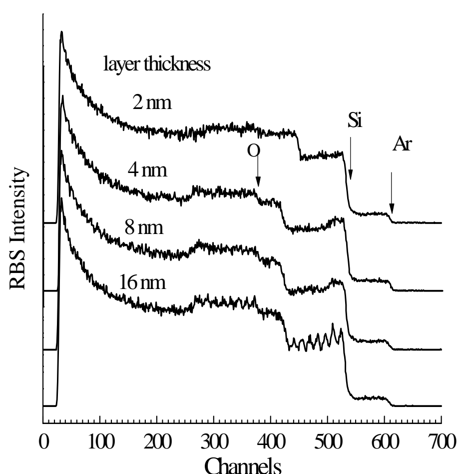

Fig. 3. Conventional RBS spectra of a-Si/SiO_2 multilayered structure. The total thickness of the stack is 256nm and the layer thickness is indicated on each spectrum.

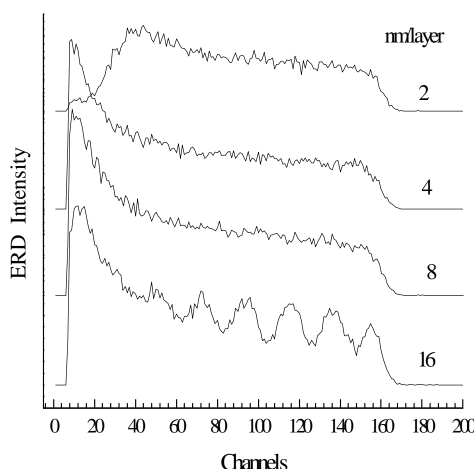

Fig. 4. Oxygen spectra obtained by ERD measurements for samples with RBS spectra in Fig. 3.

Using HR-RBS the composition of each layer from the multilayered stack can be determined. The results of these measurements are presented in figure 5 where the structure of the first 18 nm depth is resolved. The measurement conditions were chosen in such a way to have both the Si and the O signal in each spectrum. This is very helpful in the simulation process. The RUMP fit for each spectrum gives the composition and the thickness of the layers as they are presented in Table 1. We firstly note that the results of conventional RBS and ERD are confirmed: the composition of "SiO_2" layers is altered and SiO_x (with $x<2$) is obtained for layer with thickness up to 4 nm. Thus instead of 2 oxygen atoms per 1 silicon atom (which is normal for SiO_2) an average of 1.3 oxygen atoms for "SiO_2" 4 nm/layer and 0.8 oxygen atoms for 2 nm/layer was obtained. This means that the oxygen amount necessary to built SiO_2 was not reached in a "SiO_2" deposition time of 20 sec and 10 sec respectively (SiO_2 rate deposition is 12 nm/min) . We have to note that these depositions were made with continuously silicon sputtering and the oxygen line was "opened" and "closed" at the right moment to grow SiO_2 layers of desired thicknesses. When the oxygen atoms reach the deposition surface the oxidation reaction is immediate, taking into account the reactivity of both the oxygen atoms and the new deposition surface. The Si spectrum of a-Si layer (see Fig. 5) is slightly asymmetric: the edge that corresponds to the moment of "close" the oxygen line is steeper than the edge of "open". The RUMP simulation reveals that this is a straggling effect.

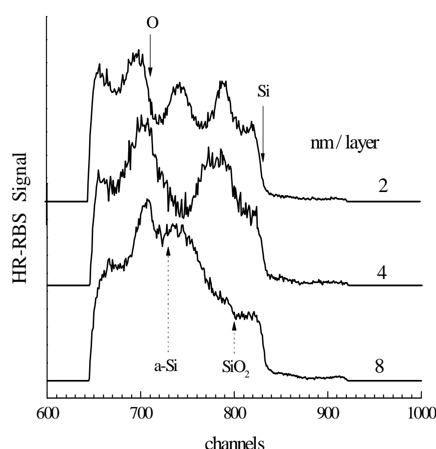

Fig. 5. HR-RBS spectra of samples with 2, 4 and 8 nm/layer. The multilayered structure is shown in the Si depth profile. On the top of the 3-rd a-Si layer (2nm) is the O profile from the 1-st SiO_2 layer .

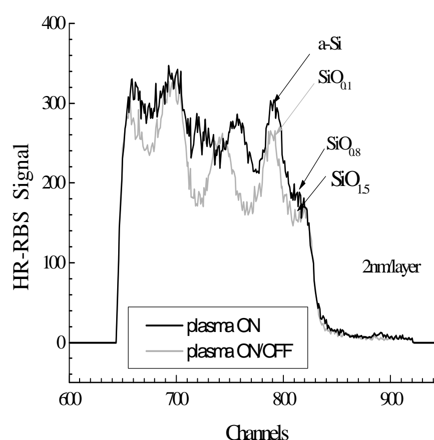

Fig. 6. A comparison of 2 nm/layer samples deposited by "plasma on" and "plasma on/off" procedures. With "plasma on/off" the O amount in "SiO_2" layer increases, but there is O in a-Si layers, too.

In order to obtain more information about the deposition process of SiO_2 films with a layer thickness up to 4 nm we have repeated the deposition of samples with 4 nm and 2 nm/layer but for each layer the deposition was separately started ("plasma on/off" procedure). A comparison of HR-RBS spectra of 2 nm/layer samples deposited by the two procedures described above is shown in figure 6. Large differences can be observed:

- in "plasma on/off" there is an oxygen contamination of the a-Si layers, and
- the "SiO_2" layers are richer in oxygen than the similar "plasma on" layers ($SiO_{1.4}$ instead of $SiO_{0.8}$).

Table 1. The composition and the areal thickness for each layer from the a-Si/SiO_2 stacks obtained fitting HR-RBS spectra.

			8 nm/layer		4 nm/layer		2 nm/layer	
Layer nr	Si	Ar	Thickness (at. cm^{-2})	O	Thickness (at. cm^{-2})	O	Thickness (at. cm^{-2})	O
1	1	0.05	$30 \cdot 10^{15}$	2	$15 \cdot 10^{15}$	1.3	$13 \cdot 10^{15}$	1.2
2	1	0.03	$26 \cdot 10^{15}$	0	$14 \cdot 10^{15}$	0	$6 \cdot 10^{15}$	0
3	1	0.05			$14 \cdot 10^{15}$	1.3	$9 \cdot 10^{15}$	0.8
4	1	0.03			$14 \cdot 10^{15}$	0	$5.5 \cdot 10^{15}$	0
5	1	0.05			$12 \cdot 10^{15}$	1.2	$7 \cdot 10^{15}$	0.8
6	1	0.03					$6 \cdot 10^{15}$	0
7	1	0.05					$9 \cdot 10^{15}$	0.8
8	1	0.03					$7 \cdot 10^{15}$	0
9	1	0.05					$9 \cdot 10^{15}$	0.8

The amount of 10% oxygen in a-Si layers is the result of the oxidation of the Si surface after the oxygen line was opened while the plasma was switched off. An oxygen rich very thin layer is formed at the surface, during the pumping time. Oxygen molecules are also adsorbed on the vessel walls and sputter target during the growth of SiO_2 layers. When the deposition of the new a-Si layer starts, the sputtering process will begin with an oxidized surface of the target. These are the oxygen sources which could explain the oxygen content from the front edge of silicon spectrum. When the a-Si deposition is finished, the silicon surface is very reactive. Between the moment when the gases for the SiO_2 layer are introduced in vessel and the moment when plasma is in equilibrium conditions there is a period of time when high concentration oxygen is built on the surface. The ion bombardment and/or the oxidation process will determine silicon atoms to "diffuse" towards the new surface. In this way the a-Si layers deposited in "plasma on/off" procedure are thinner than that deposited in "plasma on".

3.2. Defects: ESR

An ESR experiment reveals the paramagnetic defects from the sample. Generally the derivative absorption of microwave power is measured as a function of the magnitude of an externally applied magnetic field. In Fig 8 the spectrum of the samples with 8 nm/layer is shown. As can be seen two types of defects are present and they are characterized by their g factor values /8/. The defect density and the g values associated with these defects are obtained by deconvolution of the spectra using two Lorentzian lineshapes. They are shown in table 2. We note that a g value of 2.0055 is assigned to a-Si dangling bond defects (DB) while 2.0012 is due to E' defects from SiO_2 /8/. As can be seen from the table2, the a-Si DB defects are identified. Their density of spins increases when the individual layer thickness decreases. The g values that we found for this type of defect are smaller (2.0048 instead of 2.0055) because of oxygen surroundings. Concerning the second type of defects, the g value associated slightly increases and its Lorentzian line becomes broader for thinner layer in the stack. This can be due to different surroundings of $O_3{\equiv}Si{\cdot}$- defect entity /9/. Very interesting is the evolution of the density of spins associated with this defect: it decreases for the sample with 4 nm/layer and can not be detected for that with 2 nm /layer. This is in good agreement with the results of HR-RBS where no SiO_2 was found for those samples. However it should be noted that using ESR only minority sites concerning defects are detected. The lack of $O_3{\equiv}Si{\cdot}$- defects could also indicate a more preferential existence of defects near Si clusters. As it is shown in /10/, by varying the microwave power we have reached the value where the E' defects were saturated. This experiment has allowed us a better separation between the two defects types.

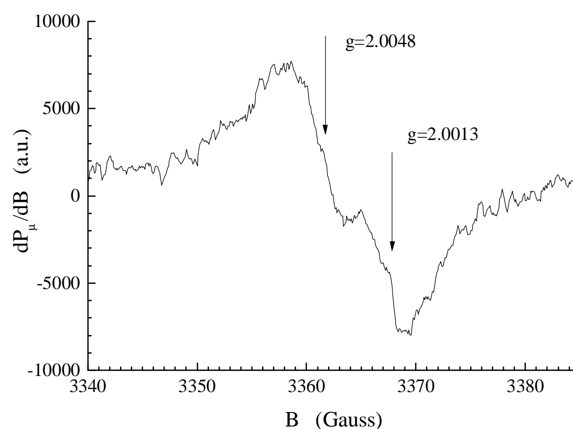

Fig. 7. ESR spectrum of multilayered samples with 8 nm/layer. With arrows are indicated the a-Si DB and E' contributions at the spectrum

Tabel 2. The values of the g factor and the spin density as they result from the ESR spectra analysis.

Thickness (nm/layer)	g_1	g_2	n_{s1} (spins/cm^3)	n_{s2} (spins/cm^3)
8	2.00486	2.00138	$2.82 \cdot 10^{20}$	$8.74 \cdot 10^{19}$
4	2.00474	2.00158	$2.99 \cdot 10^{20}$	$4.54 \cdot 10^{19}$
2	2.00486	-	$5.73 \cdot 10^{20}$	-

4. Conclusions

From the results on our a-Si/SiO_2 multilayered samples we summarize:

i) The ion beam analysis techniques are competitive to determine the stoichiometry and the areal thickness of thin layers. Conventional RBS and ERD reveal layers with geometrical thickness larger than 16 nm. Best results are obtained using a combination of both RBS (for elements with larger atomic mass) and ERD (for elements with smaller mass) and to correlate their results in the region of the mass where the two techniques overlap.
High resolution RBS using a magnetic spectrograph has revealed layers with a thickness of 2 nm.

ii) With our sputtering deposition system we used two procedures in order to obtain layers as thin as possible of a-Si and SiO_2. The thinnest a-Si layer in a stack of a-Si/SiO_2 which is resolved by HR-RBS is 2nm while for SiO_2 we found 4 nm.

iii) The deposition procedure "plasma on/off" gives higher oxygen concentrations in "SiO_2" layer from the stack, but introduces also a small amount of oxygen in a-Si layers.

iv) ESR measurements show a convolution of two Lorentzian absorption lines. One of this can be identified as defects in silicon reach environment and the other one seems to be associated with defects in SiO_2 clusters.

References

[1] S. A. Fayek, A. F. Maged, M. R. Balboul, Vacuum **53**, 447, (1999).
[2] D. R. Hamann, Phys. Rev B **122**, 9899, (2000).
[3] L. C. Feldman, J. W. Mayer, Fundamentals of Surface and Thin Film Analyses, North-Holland, New York, 1986.

[4] J. F. Ziegler, J. P. Biersack, U. Littmark, The stopping and range of ions in solids Pergamon Press Inc., New York, 1985 (reviewed in 1990).
[5] L. R. Doolittle, Nucl. Instr. & Methods, **B9**, 344 (1985).
[6] G. F. Knoll, Radiation Detection and Measurements, 3-rd ed., John Wiley and sons, 152, 2000.
[7] W. M. Arnoldbik, W. Wolfswinkel, D. K. Inia, V. C. G. Verleun, S. Lobner, J. A. Reiders, F. Labohm, D. O. Boerma, Nucl. Instr. and Meth. in Phys. Research, **B118**, 566 (1996).
[8] M. Lannoo, P. Friedel, Atomic and Electronic Structure of Surfaces, Editor M. Cardona, Springer - Verlag, 196, 1991.
[9] W. L. Warren, E. H. Poindexter, M. Offenberg, W. Muller-Warmuth, J. Electrochem. Soc., 139, 872 (1992).
[10] N. Tomozeiu, E. E van Faassen, A. M. Vredenberg, F. H. P. M. Habraken, to be published in ICAMS 19-th Proceedings (J. Non-Cryst. Sol.).